Original Article
Endoplasmic reticulum stress triggers delanzomib-induced apoptosis in HCC cells through the PERK/eIF2α/ATF4/CHOP pathway

Jun Li[1,3,4,5,6], Jian-Yong Zhuo[2,3], Wei Zhou[2,3], Jia-Wei Hong[2,3], Rong-Gao Chen[2,3], Hai-Yang Xie[2,3,4,5,6], Lin Zhou[2,3,4,5,6], Shu-Sen Zheng[2,3,4,5,6], Dong-Hai Jiang[2,3,4,5,6]

Departments of [1]Clinical Pharmacy, [2]Surgery, Division of Hepatobiliary and Pancreatic Surgery, First Affiliated Hospital, School of Medicine, Zhejiang University, Hangzhou 310000, Zhejiang Province, China; [3]NHFPC Key Laboratory of Combined Multi-Organ Transplantation, Hangzhou 310000, Zhejiang Province, China; [4]Key Laboratory of The Diagnosis and Treatment of Organ Transplantation, CAMS, China; [5]Key Laboratory of Organ Transplantation, Hangzhou 310003, Zhejiang Province, China; [6]Collaborative Innovation Center for Diagnosis Treatment of Infectious Diseases, Hangzhou 310000, Zhejiang Province, China

Abstract: For limited clinical benefits and acquired resistance by sorafenib, new therapeutic strategies and molecular targets for the treatment of advanced hepatocellular carcinoma (HCC) are urgently needed. This study aimed to evaluate the potential antitumor effects of the second-generation proteasome inhibitor delanzomib on HCC. The results demonstrated that delanzomib displayed excellent antitumor activity on HCC cells with sensitivity or resistance to sorafenib in a time- and dose-response manner, by inducing G2/M cell cycle arrest and apoptosis in vitro. Cell cycle arrest was associated with the activation of p21/Cdc2/cyclin B1 pathway, and cell apoptosis was confirmed by PARP and caspase-3 cleavage. In addition, delanzomib induced endoplasmic reticulum stress (ERS) in HCC cells by activating the PERK and ERS-associated proteins including p-eIF2α, ATF4 and CHOP. Selective inhibition of eIF2α dephosphorylation by salubrinal could significantly reduce delanzomib-induced apoptosis in HCC cells. In vivo, delanzomib could also exhibit effective antitumor properties on patient-derived xenograft mouse model of HCC with relative low drug-associated cytotoxicity. Compared to control group, 3 and 10 mg/kg of delanzomib significantly reduced the tumor volume by 33.1% and 87.2% respectively after 3 weeks treatment, with no significant change on the body weight and the level of serum biochemical indexes including ALT, AST and BUN. In conclusion, delanzomib could exhibit good pre-clinical antitumor effects against HCC cells by inducing ERS and activating the PERK/eIF2α/ATF4/CHOP pathway, as potential drug candidate on treatment of advanced HCC patients.

Keywords: Delanzomib, HCC, apoptosis, endoplasmic reticulum stress, sorafenib resistance

Introduction

Hepatocellular carcinoma (HCC) is the second most frequent solid tumor and the third leading cause of cancer related death all over the world [1]. And this situation is more severe in far eastern countries [2]. Surgery is the most effective treatment for the early stages of HCC, but over 70% of HCC patients are already in the advanced stage under the first diagnose, without indication for surgical resection [3]. Sorafenib is the standard treatment regimen for advanced HCC [4]. However, its survival benefit is only 3 months with many side effects [5].

Moreover, HCC relapse is quickly even for the initial responders to sorafenib [6]. Therefore, there is an urgent need for development of new therapeutic strategies and identification of new molecular targets for advanced HCC patients.

Proteasome inhibitor is a series of molecular targeted agents used to prevent the degradation of pro-apoptotic factors and lead the accumulation of misfolded proteins, which might trigger the activation of the apoptotic pathway and promote the programmed death of cancer cells [7]. Previous studies identified the link between abnormal proteasome activity and

HCC progression, and proteasome inhibitors were considered to be potential agents for HCC treatment [8]. Bortezomib, a first-generation proteasome inhibitor approved by FDA for treatment of multiple myeloma (MM) [9, 10], has demonstrated as anti-proliferative and pro-apoptotic effects on HCC in pre-clinical researches [8]. However, a multi-center single-arm phase II study in patients with nonsurgical or metastatic HCC showed that bortezomib could be well tolerated, but lacked significant clinical efficacy [11]. And the mechanisms was not fully elucidated yet [8].

On the other hand, the next-generation proteasome inhibitors have been developed for further improving the drug efficacy, minimize the toxicity and avoid resistance on treatment of hematologic tumors. Among them, delanzomib (CEP-18770), a second generation reversible proteasome inhibitor, produces cytotoxic effects via inhibiting chymotrypsin-like activity of the proteasome with a significantly lower IC50 value compared to other proteasome inhibitors [12]. Followed with administration of the equivalent doses, delanzomib demonstrated greater and more sustained binding to the β5/β1 proteasome subunits than bortezomib, with 86% inhibition of the proteasome activity compared with 48% for bortezomib [12, 13]. More interestingly, delanzomib overcame the acquired bortezomib-resistance originated from a mutation in β5 subunit protein in vitro [14]. In vivo, delanzomib could also produce antitumor effects on bortezomib-resistant MM cells, and the additional delanzomib induced a substantial delay on the disease progression of bortezomib-resistant tumors [15].

However, no studies were conducted to evaluate the antitumor effects of delanzomib on HCC. And whether delanzomib remains active in sorafenib-resistant HCC cells was still unclear. Herein, we speculated that delanzomib could exhibit excellent antitumor effect on HCC cells by inducing G2/M cell cycle arrest and cell apoptosis in vitro, and significantly suppressed the HCC tumor growth in vivo with relative low systemic cytotoxicity. Moreover, delanzomib could induce endoplasmic reticulum stress (ERS) in HCC through activating the PERK and subsequent ERS-associated proteins including p-eIF2α, ATF4 and CHOP. Interestingly, sorafenib-resistant HCC cell remained sensitive to delanzomib.

Material and methods

Chemicals and reagents

Delanzomib was purchased from Meilun Biotechnology (Dalian, China) and dissolved in DMSO as the 10 mM stock solutions for application. Working solutions were prepared by diluting the stock solution to the indicated concentrations immediately before treatment. The final concentration of DMSO is less than 0.1% in all experiments. Salubrinal was purchased from Beyotime Biotechnology (Shanghai, China). Primary antibodies against PARP (#9532), Cleaved PARP (#32563), Cleaved caspase-3 (#9664), P21 (#2947), Cdc2 (#28439), p-Cdc2 (#4539), Cyclin B1 (#4135), PERK (#56-83), eIF2α (#2103), CHOP (#2895) and β-actin (#4970) were purchased from Cell Signaling Technology (Danvers, MA, USA). p-PERK (ab19-2591), p-eIF2α (ab32157), ATF4 (ab184909) and anti-Ki67 antibodies (ab15580) were purchased from Abcam (MA, USA).

Cell culture

Human HCC cell lines HCC-LM3, SK-hep-1, SUN-449, HepG2 and human normal liver cells LO2 were obtained from China Center for Type Culture Collection (CCTCC). Immortalized porcine hepatocyte line HepLi was kindly provided by Prof. Lanjuan Li of Zhejiang University. All cell lines were cultured in minimum essential medium (MEM, Gibco-Invitrogen, USA) supplemented with 10% fetal bovine serum and antibiotics (100 U/ml penicillin and 100 μg/ml streptomycin), in humidified air at 37°C with 5% CO_2. Sorafenib-resistant HCC cell line (SK-sora-5) was established in our laboratory based on continuous exposure to sorafenib using a dose-stepwise incremental strategy from SK-hep-1 as described in our previous publication [16], and maintained in medium containing 5 μM sorafenib before all experimental procedures.

Mice

Female aged 4 weeks of athymic nude (nu/nu) mice and NOD/SCID mice were purchased from Shanghai SLAC animal facility. Animals were housed in a specific pathogen-free (SPF) mouse facility at the animal centre of the first affiliated hospital, Zhejiang University. All animals care and experiments were conducted according to

the guidelines of Zhejiang university animal care committee.

MTT assay

To assay the anti-proliferation effect of delanzomib, cells were suspended at a final concentration of $1×10^4$ cells/ml and seeded in 96-well tissue culture plates. After one night of incubation, the designated columns were treated with drug regimes. Four hours prior to the end of time point, MTT solution (5 mg/ml) was added. The formazan crystals were dissolved in 150 μL DMSO after 4 h incubation and the optical densities at 570 nm were measured with a universal microplate reader (Bio-Rad, Sunnyvale, CA).

Colony-forming assay

Cells were seeded into 60-mm tissue culture dishes in triplicates at a density of 1000 cells/dish and cultured in a humidified incubator at 37°C with 5% CO_2 overnight. Then, the cells were incubated with or without delanzomib for about two weeks until colonies were visible. The cell colonies were stained with giemsa.

Analysis of cell cycle

Cell cycle distribution was assessed by flow cytometric analysis. Briefly, after drug exposure for 48 h, both detached and attached cells were harvested and washed twice with cold phosphate buffer solution (PBS), and then fixed in 75% ethanol. Prior to analysis, cells were washed again and incubated in PBS containing 100 μl/ml RNase and 40 μl/ml propidium iodide (PI) at room temperature for 0.5 h. Cell cycle distribution was determined using a Coulter Epics V instrument (Beckman Coulter, FL, USA).

Analysis of apoptosis

Cell apoptosis was analyzed using the Annexin V-FITC/PI apoptosis detection kit according to the manufacturer's instruction (Beyotime, Shanghai, China). Briefly, cells were harvested and washed twice with cold PBS after treatment with different concentrations of delanzomib for 48 h. Then the cells were suspended with 400 μl of binding buffer, 5 μl of Annexin V antibody conjugated with fluorescein isothiocyanate (FITC) and 5 μl of PI solution. After being stained in the mixture for 15 min at room temperature in the dark, apoptotic cell ratio was detected by flow cytometry (Beckman Coulter, FL, USA).

Western blot analysis

Total protein was obtained by lysing cellular sample in cold RIPA buffer (50 mM Tris-HCl [pH 8.0], 150 mM NaCl, 0.1% SDS, 0.5% sodium deoxycholate, 1% Triton-X100, 1 mM EDTA) with 1% protease and phosphatase inhibitor cocktail (Beyotime, Shanghai, China). Equal amounts (30 μg/lane) of proteins were separated by electrophoresis on a 12% SDS-PAGE gel and transferred to nitrocellulose membranes (Millipore, USA) following conventional protocols. Before immunoblotted, membranes were blocked in 5% non-fat milk in Tris-buffered saline containing 0.1% (v/v) Tween 20 at room temperature for 1 h. Then, the membranes were incubated overnight at 4°C with the primary antibodies described in section "Chemicals and reagents". Protein bands on the membranes were detected by incubating with horseradish peroxidase (HRP) conjugated antibodies. Immunoreactive bands were visualized using ECL kits in accordance with the manufacturer's instructions (Abcam, MA, USA). β-actin levels were also analyzed as controls for protein loading.

Patient-derived xenograft (PDX) mouse model

HCC tissue for PDX model was obtained from the first affiliated hospital of Zhejiang University. The patient was asked informed consent according to the regulation concerning human samples in the first affiliated hospital of Zhejiang University. PDX model was established as previous publication described [17]. Fresh tumor tissue was incubated in ice-chilled high-glucose DMEM with 10% FBS, 100 U/ml penicillin and 100 μg/ml streptomycin and processed rapidly for engraftment. After the removal of necrotic tissue, the tumor specimens were partitioned into 2 mm^3 sections approximately and transplanted into the right flanks of NOD/SCID mice (female, 5-6 weeks old) subcutaneously with a no. 20 trocar under aseptic conditions. Once the diameter of the subcutaneous tumor reached 1 cm, it was partitioned into pieces (about 2 mm^3) and then subcutaneously implanted into the flanks of 4-5 weeks old athymic nude mice. Three days after implantation, the mice were randomly divided into 3 groups and treated with different

regimens based on previous studies [12, 15]: (1) vehicle; (2) delanzomib at 3 mg/kg and (3) delanzomib at 10 mg/kg (n=6 per group). The treatment regimens were repeated twice weekly (W, F) via IV injection for 3 weeks in a volume of 10 ml/kg body weight of mice. The body weight and tumor volume of mice were measured twice every week until the animals were terminated. Tumor size was measured using a caliper. Tumor volume was calculated using the formula: tumor volume = length × (width)^2 × 0.5. After the animals were terminated, the tumor tissue samples from mice were isolated and weighted. All experiment protocols were approved by the research ethics committee of the first affiliated hospital, Zhejiang University (No. 2017-720).

Immunohistochemical staining and TUNEL assay

Immunohistochemistry analysis was carried out as previously described [18]. Briefly, tumor tissues and organs (liver and kidney) were fixed in 10% formalin, paraffin-embedded, sliced, and collected on coated slides for HE staining. Ki-67 staining was performed after dewaxing and rehydration of tumor sections on slides. TUNEL assay with situ cell death kit was adopted for analysis of the apoptosis induction in the tumor tissue specimen as the manufacturer's instructions (Meilun, Dalian, China).

Biochemical indexes detection

Routine biochemical indexes including alanine aminotransferase (ALT), aspartic aminotransferase (AST) and blood urea nitrogen (BUN) were analyzed in serum samples of mice by automatic biochemical analyzer (Mindray BS-800, China).

Statistical analysis

All experiments were performed in triplicate unless otherwise noted. Results were presented as mean ± standard deviation (SD). Comparisons between two groups were made using one-way analysis of variance (ANOVA) followed by Dunnett's test by statistical software SPSS version 22.0 (SPSS, Chicago, IL, USA). *P* value less than 0.05 was considered to be statistically significant.

Results

Delanzomib preferentially inhibits HCC cells proliferation compared with normal liver cells

To explore the effect of delanzomib on HCC cells proliferation, MTT assay was adopted to examine the cell viability on four HCC cell lines (HCC-LM3, SK-hep-1, SUN-449 and HepG2) and two normal liver cells (LO2 and HepLi). As shown in **Figure 1A**, delanzomib substantially inhibited HCC cells proliferation, and the IC50 values of HCC cell lines after treatment with delanzomib for 72 h were all below 30 nM, ranged from 7.4 nM to 29.8 nM. However, the IC50 values of delanzomib on normal liver cells LO2 and HepLi were 152.7 nM and 168.5 nM respectively and significantly higher than HCC cell lines (P<0.001). Meanwhile, we selected HCC-LM3 cells with the most sensitivity as an example. Delanzomib inhibited HCC-LM3 cell proliferation in a time- and dose-dependent manner (**Figure 1B**). Morphological observation showed that delanzomib significantly affected the shape and reduced the adhesive force of HCC-LM3 cells in comparison with control group after treatment with delanzomib (10 nM and 20 nM) at 48 h. A typical morphological feature of apoptotic cells could also be observed, and cells became rounded and detached from the substrate as shown in upper panel of **Figure 1C**. Moreover, compared to the control group, HCC-LM3 cells showed fewer and smaller colonies after being treated by delanzomib (upper panel of **Figure 1D**). However, these phenomenons were not observed in normal liver cells (lower panels of **Figure 1C**, **1D**).

Delanzomib induces G2/M cell cycle arrest and apoptosis in HCC cells

To clarify delanzomib-induced anti-proliferation effect on HCC cells, the cell cycle phase distributions of HCC-LM3 cells was examined by flow cytometry analysis. As shown in **Figure 2A**, after treatment with 10 nM and 20 nM of delanzomib for 48 h, the proportion of cells at G2/M phase increased significantly from 20.7% to 37.0% and 52.1% (P<0.05), respectively. Furthermore, a detailed analysis of the proteins expression involved under the control of G2/M phase in cell cycle progress was conducted. Treatment with delanzomib for 48 h resulted in
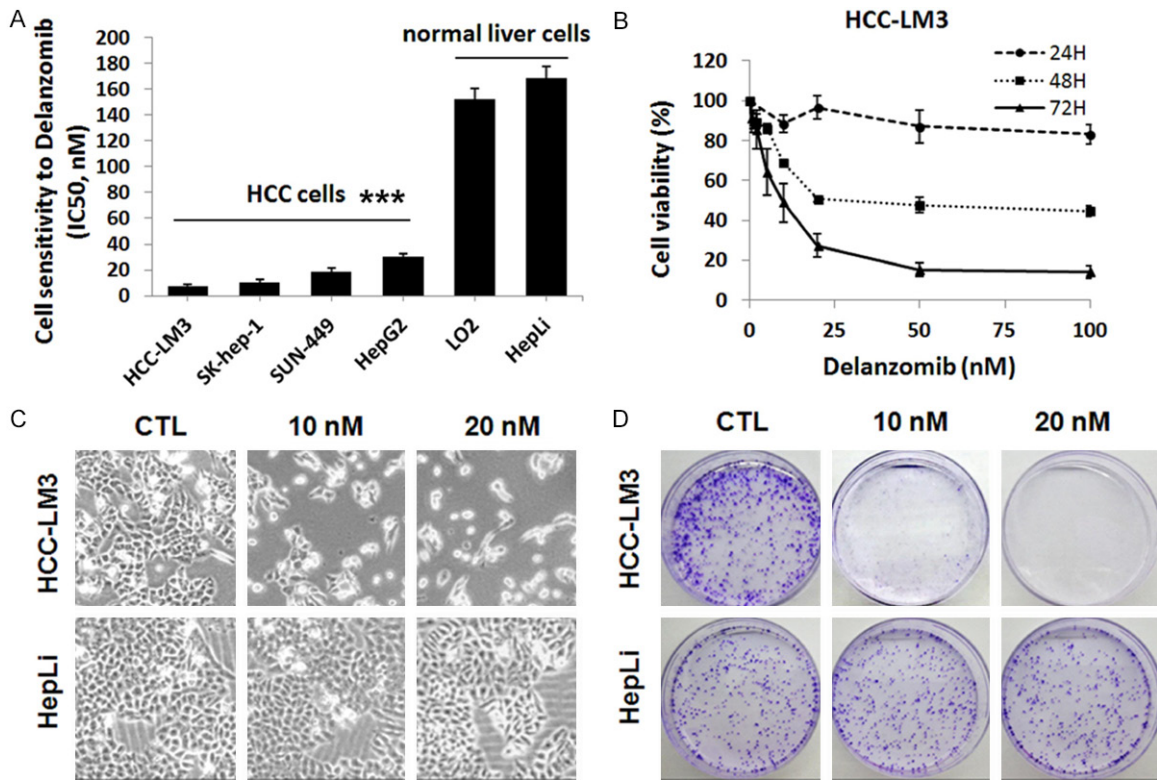
Figure 1. Delanzomib preferentially inhibits HCC cells proliferation compared with normal liver cells in vitro. A. The IC50 values of delanzomib were determined for each HCC cell lines and normal liver cell lines after treatment for 72 h. B. HCC-LM3 cells were treated with increasing doses of delanzomib for indicated time, and cell viability was assessed by the MTT assay. C. Morphological observation of HCC-LM3 and HepLi cells after treated with 10 and 20 nM of delanzomib for 48 h by an inverted microscope under 40× magnification. D. Colony formation of HCC-LM3 and HepLi cells after treatment with or without delanzomib. Data are presented as mean ± SD from three independent experiments. ***P<0.001 HCC cells vs. normal liver cells. CTL, control.

an increased expression of the inhibitor of cyclin-dependent kinase p21 and a decrease expression on Cdc2, pCdc2 and cyclin B1 protein levels (**Figure 2C**) (The Original image of WB scan is shown in the Supplementary Figure 1).

Moreover, annexin V-FITC and PI staining were used to assess cell apoptosis. As shown in **Figure 2B**, compared with controls, the ratio of apoptotic cells significantly increased from 3.2% to 9.8% and 18.5% after being exposed to 10 nM and 20 nM of delanzomib for 48 h in HCC-LM3 cells (P<0.05), respectively. In addition, delanzomib exposure lead to a stronger cleavage of poly ADP-ribose polymerase (PARP) and caspase-3 (**Figure 2D**) (The Original image of WB scan is shown in the Supplementary Figure 2).

Sorafenib-resistant HCC cell remained sensitive to delanzomib

Acquired resistance limited the clinical efficiency of sorafenib. In order to illuminate whether delanzomib remained active in sorafenib-resistant HCC cells, a sorafenib-resistant HCC cell line (SK-sora-5) was established based on continuous exposure to sorafenib using a dose-responsed incremental strategy from SK-hep-1 as described in our previous publication [16]. The sensitivities of SK-hep-1 and SK-sora-5 to sorafenib were examined. The IC50 values after treatment with sorafenib for 72 h were 3.81 and 8.46 µM, respectively (P<0.01, **Figure 3A**). Interestingly, delanzomib inhibited cell proliferation in a time- and dose-dependent manner without significant difference between two cell lines (**Figure 3B**, **3C**). The IC50 of delanzomib to SK-hep-1 and SK-sora-5 after treatment
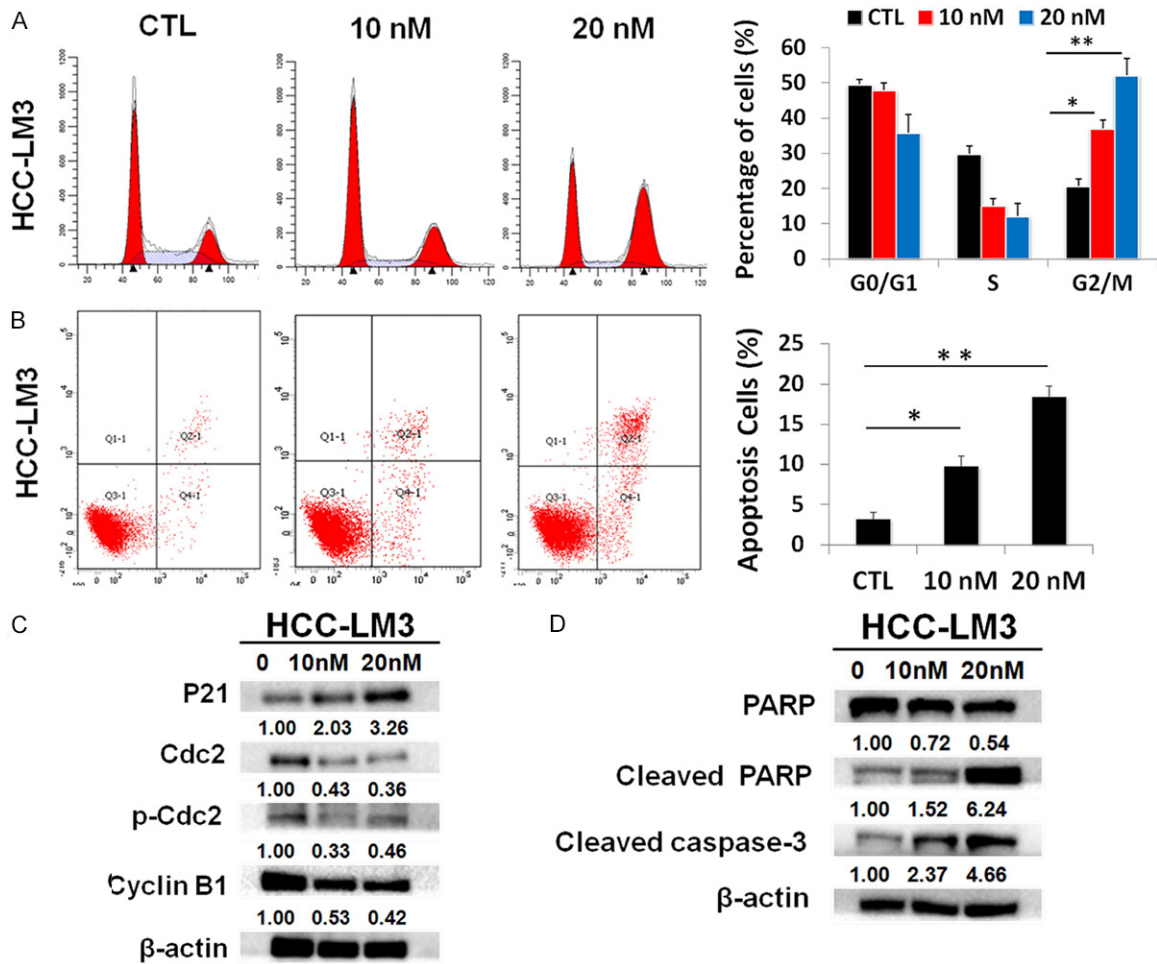
Figure 2. Delanzomib induces G2/M cell cycle arrest and apoptosis in HCC-LM3 cells. (A) After treated with delanzomib as indicated concentrations in HCC-LM3 cells for 48 h, the cell cycle phase distribution was analyzed after staining with propidium iodide by flow cytometry, and the data of cell cycle distribution was summarized. (B) Cell apoptosis was assessed by Annexin V-FITC/PI flow cytometry analysis and the data of apoptotic percentage was summarized. Western blot analysis of p21, Cdc2, pCdc2 and Cyclin B1 proteins for cell cycle arrest (C) and PARP, Cleaved PARP, Cleaved caspase-3 proteins for cell apoptosis (D) were conducted after treatment with delanzomib for 48 h. β-actin was analyzed as control for protein loading. Number indicated relative abundance (arbitrary unit). Data are presented as mean ± SD from three independent experiments. *P<0.05; **P<0.01. CTL, control.

for 24, 48 and 72 h were 51.3, 15.8, 10.7 nM vs. 46.3, 18.8 and 13.1 nM, respectively (P>0.05, **Figure 3D**). Morphological observation (**Figure 3E**) and colony formation assays (**Figure 3F**) also demonstrated that the antiproliferational activity of delanzomib is similar between SK-hep-1 and SK-sora-5 cells. Delanzomib (10 nM and 20 nM) significantly affected the shape and reduced the adhesive force after 48 hours' treatment, and resulted in fewer and smaller colonies than the control group of both cell lines. Moreover, after the treatment with 10 nM and 20 nM delanzomib for 48 h, the proportion of cells at G2/M phase was increased significantly from 21.6% to

33.3% and 57.0% for SK-hep-1 cell (P<0.05), and from 25.9% to 36.4% and 58.9% for SK-sora-5 cell (P<0.05), respectively (**Figure 3G**, **3H**). Meanwhile, treatment with delanzomib resulted in increment on the expression of p21 and decrement on Cdc2, pCdc2 and cyclin B1 protein levels in both sorafenib sensitive and resistant HCC cell lines (**Figure 3I**) (The Original image of WB scan is shown in the Supplementary Figure 3). Taken together, all these results further confirmed that delanzomib could effectively inhibit proliferation of HCC cells. More interestingly, it also indicated that sorafenib-resistant HCC cell remained sensitive to delanzomib.
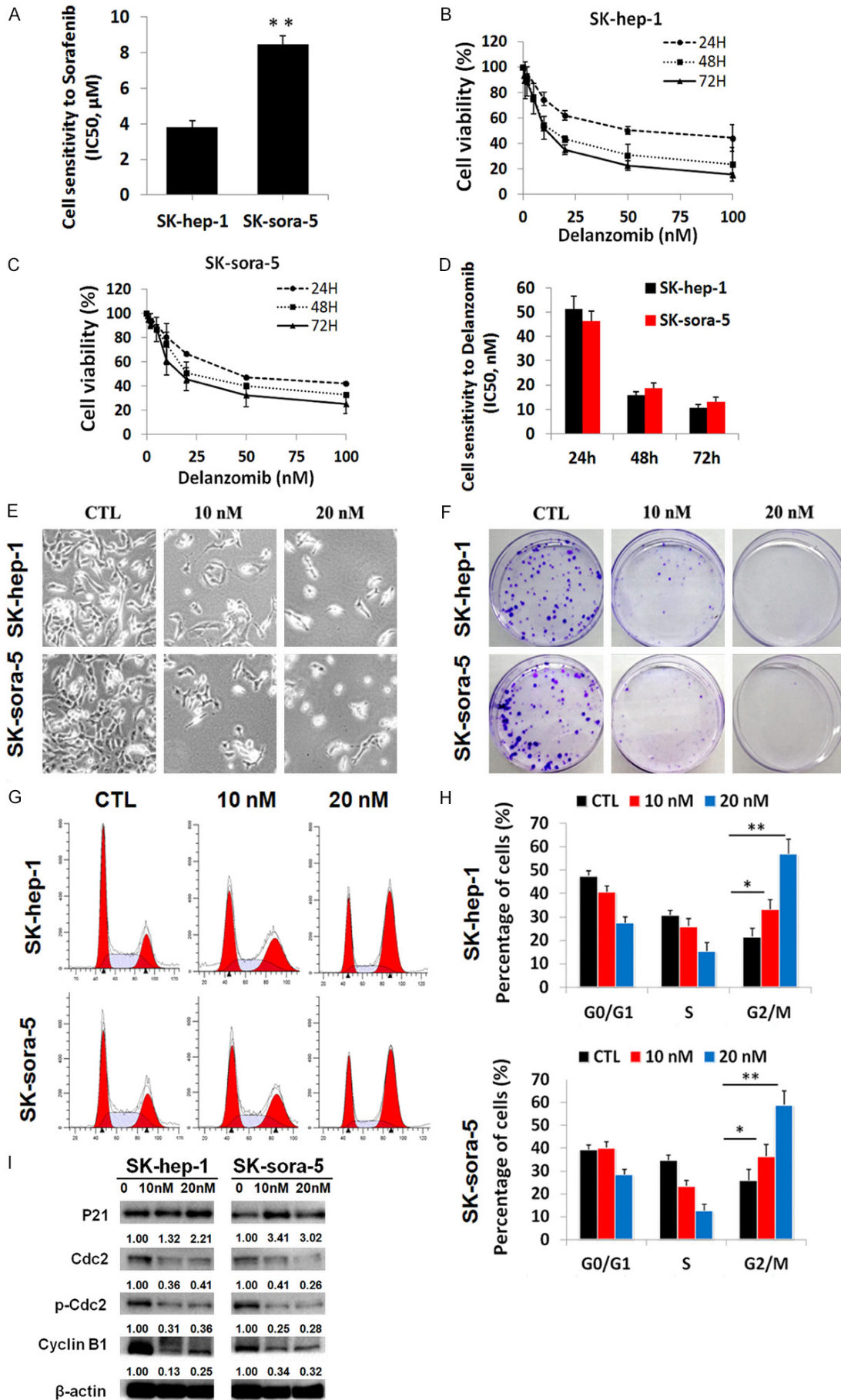
Figure 3. Sorafenib-resistant HCC cell remains sensitive to delanzomib. A. The IC50 values of sorafenib in SK-hep-1 and SK-sora-5 (a sorafenib-resistant HCC cell line) after treatment for 72 h were analyzed. B-D. After treatment with delanzomib for indicated time, cell viability of SK-hep-1 and SK-sora-5 was analyzed by MTT assay, and IC50 values were determined for both HCC cell lines. E. Morphological observation of cells after treated with delanzomib for 48 h by an inverted microscope under 40× magnification. F. Colony formation assay of SK-hep-1 and SK-sora-5 cell lines after treatment with or without delanzomib. G. Cell cycle phase distributions of both HCC cell lines were analyzed by flow cytometry after treatment with delanzomib for 48 h. H. Data of cell cycle distribution was summarized. I. Western blot was used to analyze the expression of proteins related to G2/M cell cycle arrest after treatment with delanzomib for 48 h. β-actin was analyzed as control for protein loading. Number indicated relative abundance (arbitrary unit). Data are presented as mean ± SD from three independent experiments. *P<0.05; **P<0.01. CTL, control.

ERS triggered delanzomib-induced apoptosis through PERK/eIF2α/ATF4/CHOP pathway

As shown in **Figure 4A**, delanzomib could induce apoptosis in SK-hep-1 and SK-sora-5 cells. Compared to the control group, after being exposed to 10 nM and 20 nM of delanzomib for 48 h, the percentages of apoptotic cells were increased significantly from 5.9% to 13.4% and 23.3% for SK-hep-1 (P<0.05) and from 6.1% to 11.3% and 20.5% for SK-sora-5 (P<0.05), respectively. Moreover, delanzomib could lead to a strong cleavage of PARP and caspase-3 in both cell lines on protein level (**Figure 4B**) (The Original image of WB scan is shown in the Supplementary Figure 4). For further investigate the underlying molecular mechanisms of delanzomib-induced apoptosis in HCC cells, we mainly focused on the ERS, an important mechanism for cell apoptosis based on previous reports [19, 20]. As shown in **Figure 4C**, delanzomib could up-regulate ERS-associated proteins in a concentration-dependent manner in both sorafenib sensitive and resistant HCC cells. After treatment with delanzomib on SK-hep-1 and SK-sora-5 cells for 48 h, the protein levels of p-PERK and p-eIF2α were significantly increased, whereas total PERK and eIF2α remained unchanged. Moreover, the protein levels of ATF4 and CHOP were also increased (The Original image of WB scan is shown in the Supplementary Figure 5). To further verify the role of ERS in delanzomib-induced apoptosis, salubrinal as a selective inhibitor of eIF2α dephosphorylation, was adopted to co-treated HCC cells with delanzomib. Interestingly, salubrinal significantly reduced delanzomib-induced apoptosis in both HCC cells (**Figure 4D**). The ratio of apoptotic cells decreased from 25.7% to 12.3% for SK-hep-1 (P<0.01) and from 22.8% to 11.5% for SK-sora-5 (P<0.01), respectively. All these data demonstrated that delanzomib could induce the activation of ERS, and ERS could

trigger delanzomib-induced apoptosis through the PERK/eIF2α/ATF4/CHOP pathway in HCC cells despite they were sensitive or resistant to sorafenib.

Delanzomib suppressed HCC tumor growth in PDX mouse model

In order to further verify the anti-HCC properties of delanzomib in vivo, PDX mouse model of HCC was established and administered with delanzomib (3 and 10 mg/kg) via IV injection. Compared to the control group, the tumor growth rate was significantly lower in delanzomib treated groups in a dose-dependent manner. After 3 weeks of treatment, 3 and 10 mg/kg of delanzomib treatment significantly reduced the tumor volume by 33.1% and 87.2% (P<0.05, **Figure 5A**), and tumor weight by 46.0% and 81.2% respectively (P<0.05, **Figure 5B**, **5C**). Furthermore, removed HCC xenograft tumors were tested by immunohistochemistry staining with Ki-67 and TUNEL. Compared to control group, Ki-67-positive cells were significantly decreased from 24.3% to 5.3% (P<0.01, **Figure 5D**). Correspondingly, the number of TUNEL-positive cells in tumor tissues were increased from 3.2% to 25.3% (P<0.01, **Figure 5E**) after treatment with 10 mg/kg of delanzomib for 3 weeks. These results demonstrated that delanzomib could inhibit HCC cell proliferation and induced apoptosis in vivo.

Delanzomib exhibited relative low drug-associated cytotoxicity in vivo

Furthermore, drug-associated cytotoxicity of delanzomib in vivo was monitored by analysis on body weight alterations, serum ALT, AST and BUN levels, and pathological changes of liver and kidney tissues by immunohistochemistry staining. As shown in **Figure 6A**, compared with control group, no obvious difference on body weight of mice was found after 3 weeks's treat-
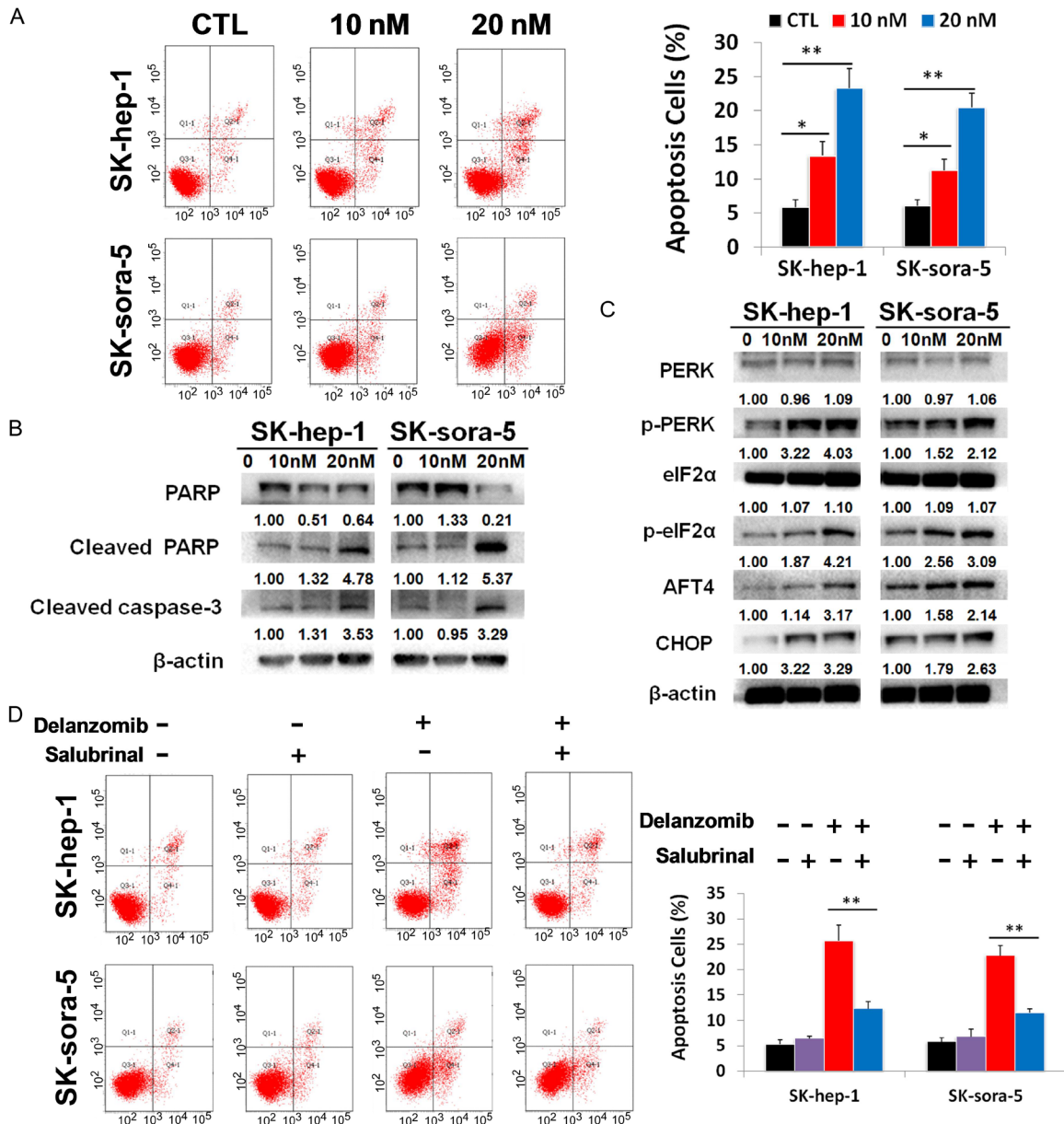
Figure 4. ERS triggers delanzomib-induced apoptosis through the PERK/eIF2α/ATF4/CHOP pathway. A. Cell apoptosis of SK-hep-1 and SK-sora-5 cell lines was assessed by Annexin V-FITC/PI analysis after treatment with delanzomib for 48 h and the data of apoptotic percentage was summarized. B. Western blot analysis of PARP and caspase-3 proteins after treatment with delanzomib for 48 h. C. SK-hep-1 and SK-sora-5 were treated with indicated concentrations of delanzomib for 48 h. The expression of PERK, p-PERK, eIF2α, p-eIF2α, ATF4 and CHOP were analyzed by western blot analysis. β-actin was analyzed as control for protein loading. Number indicated relative abundance (arbitrary unit). D. Selective inhibition of the eIF2α dephosphorylation with salubrinal could significantly reduce delanzomib-induced apoptosis in HCC cells. SK-hep-1 and SK-sora-5 cells were pretreated with salubrinal (20 μM) for 24 h before being treated with delanzomib (10 or 20 nM) for another 48 h. The cell apoptosis ratio was assessed by Annexin V-FITC/PI flow cytometry analysis. Data are presented as mean ± SD from three independent experiments. *P<0.05; **P<0.01. CTL, control.

ment of delanzomib. After removal of tumor, there was no significant difference for the net body weight of mice between each group at the end of the experiment (P>0.05, **Figure 6B**). Moreover, no significant effect was found on ALT, AST and BUN levels after treatment by delanzomib (P>0.05), and all these biochemical indexes were presented within the normal range (**Figure 6C-E**). HE staining showed that delanzomib did not cause any
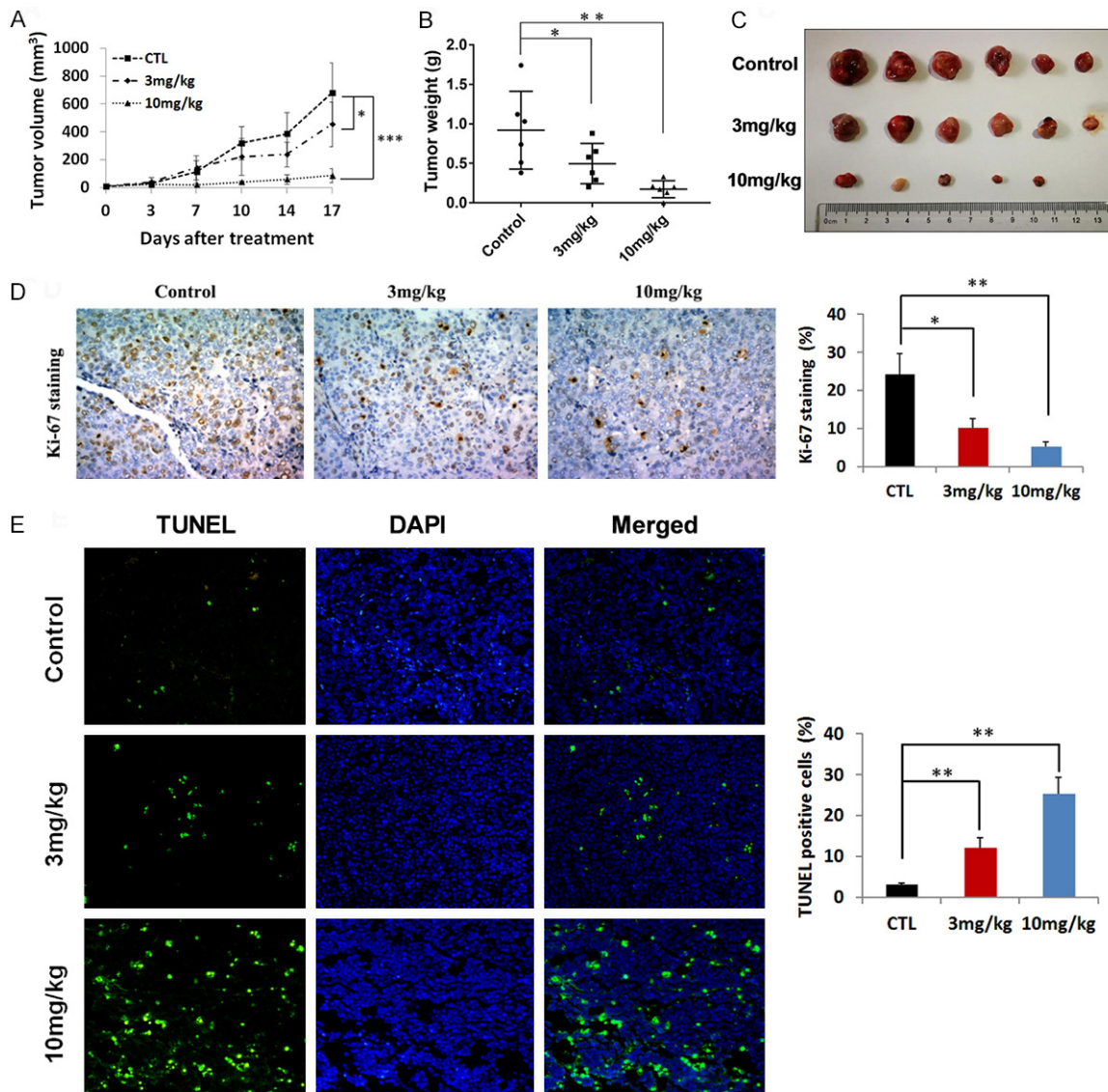
Figure 5. Delanzomib suppresses HCC tumor growth in PDX mouse model. Significant inhibition on the tumor volume (A) and tumor weight (B) at the end of experiments after 3 weeks of treatment with delanzomib at 3 or 10 mg/kg via IV injection twice weekly compared with the control group. (C) Tumor masses with or without delanzomib treatment. (D) Immunohistochemistry detected the expression levels of Ki-67 in tumor tissues (200× magnification). (E) TUNEL staining measured cell apoptosis in tumor tissues (300× magnification). Data are presented as mean ± SD (n=6). *P<0.05; **P<0.01; ***P<0.001. CTL, control.

acute injury to liver and kidney tissues either (**Figure 6F**).

Discussion

Proteasome inhibitor therapy has revolutionized the treatment of multiple myeloma, and targeting proteasomes is also considered as a promising strategy for solid tumor treatment because it selectively kills tumor cells [21]. However, although some preclinical stud-

ies have suggested that proteasome inhibition by bortezomib might be a viable therapeutic strategy for HCC [22-24], clinical results in patients with advanced HCC were disappointed [11]. Therefore, understanding the molecular basis of resistance to bortezomib in patients with HCC will aid in the development of therapeutic strategies to overcome bortezomib resistance. Current views consider that in addition to the defects on proteasome and its downstream, clinical resistance might be attrib-
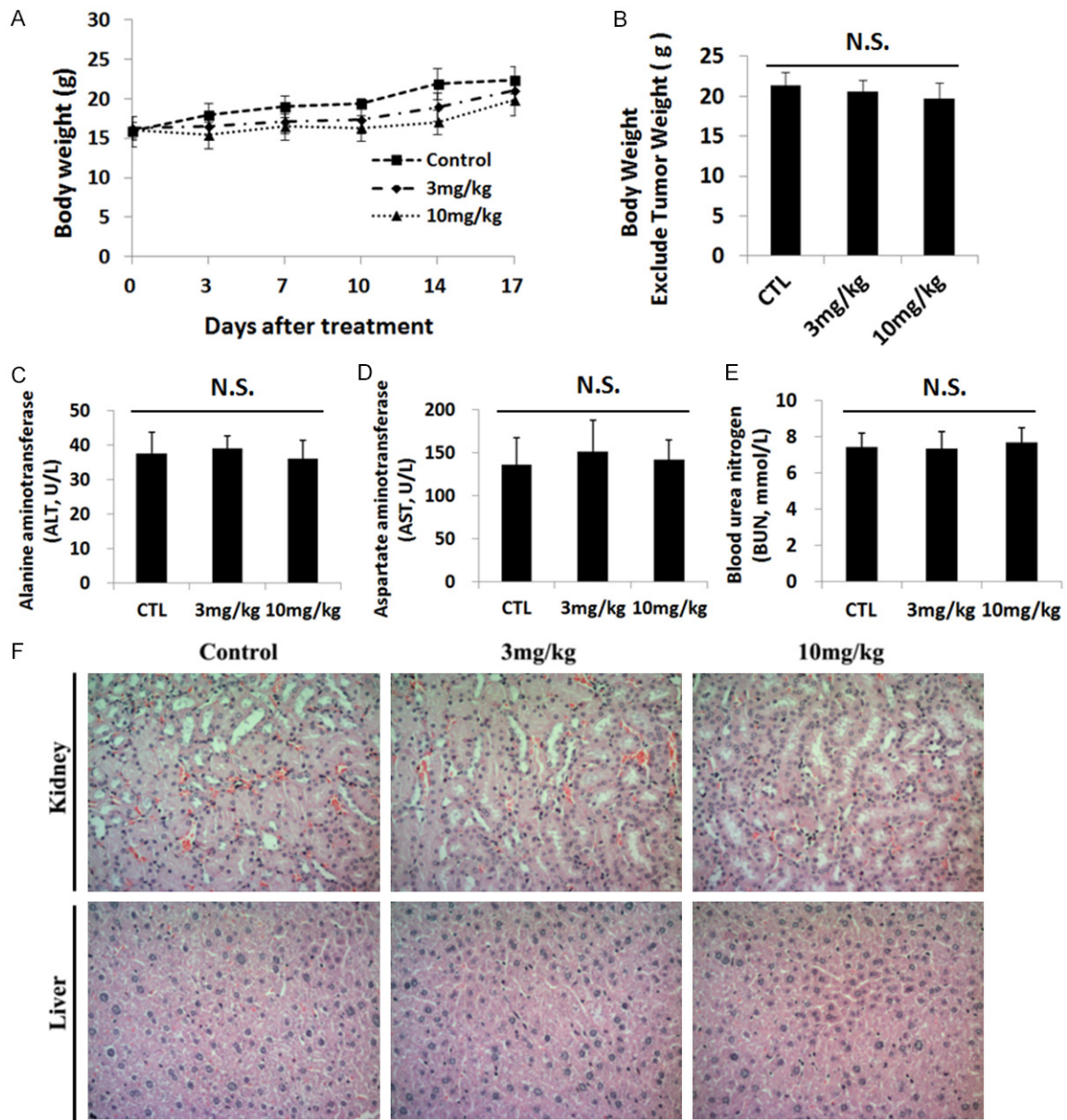
Figure 6. Delanzomib exerts relative low drug-associated cytotoxicity in vivo. A. No significant difference on body weight alterations of mice was found between different groups during 3 weeks of treatment with delanzomib. B. The net body weight of mice after tumor removal at the end of the experiment. C-E. The levels of ALT, AST and BUN in serum of mice were detected using automatic biochemical analyzer. F. HE staining was used to observe the histopathological feature of tissues, and showed that delanzomib did not cause any acute injury to liver and kidney (200× magnification). Data are presented as mean ± SD (n=6). N.S., P>0.05. CTL, control.

uted to the pharmacokinetic factors with impacts on stability, metabolism, and tissue delivery of bortezomib [25]. Previous studies demonstrated that delanzomib, a second-generation proteasome inhibitor, could inhibit tumor proteasome activity to a significantly higher extent compared to bortezomib, while delanzomib inhibited the proteasome in normal tissues

with equal potency compared to bortezomib [12, 14]. Therefore, delanzomib was adopted in the present study to analyze its potential antitumor effects on normal and sorafenib-resistant HCC cells. Our results showed that delanzomib displayed excellent antitumor effects on HCC cells in a time and dose dependent manner by inducing G2/M cell cycle arrest with activation
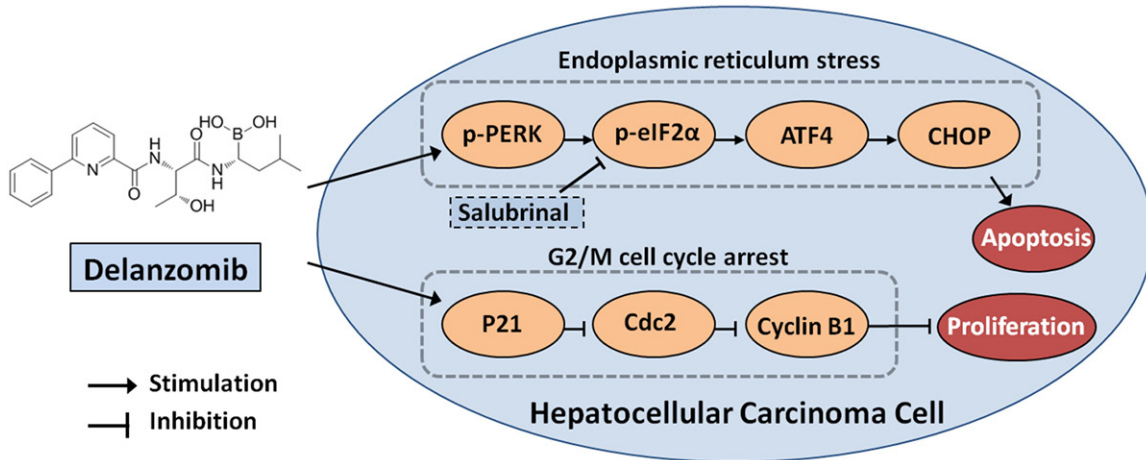
Figure 7. Schematic model illustrating the potential inhibitory mechanism of delanzomib against HCC.

on p21/Cdc2/cyclin B1 pathway and cell apoptosis with PARP and caspase-3 cleavage in vitro. Moreover, delanzomib also suppressed the HCC tumor growth in PDX mouse model with relative low drug-associated cytotoxicity in vivo. Most interestingly, delanzomib remained active in sorafenib-resistant HCC cells.

In order to further investigate the potential mechanism of delanzomib-induced apoptosis in HCC cells, we focused on the ERS on HCC cells after treatment with delanzomib. ERS, also known as unfolded protein response (UPR), was present when unfolded or misfolded proteins accumulate in the endoplasmic reticulum lumen [26]. Normally, in response to ERS, cells could up-regulate the molecular chaperones to restore protein homeostasis in the endoplasmic reticulum, either through the boosting of protein-folding and degradation capability or by assuaging the demands for such effects [27]. This response initially compensates cell damage and restores the proper homeostasis of the endoplasmic reticulum, but could ultimately activate apoptosis in response to intense or sustained ERS [28, 29]. Previous studies have shown that proteasomes play a critical role in clearing unfolded and misfolded proteins [30], and proteasome inhibitors could inhibit the degradation of misfolded proteins and trigger ERS [7]. In our present study, we also demonstrated that delanzomib could induce ERS in HCC through activating the PERK as one of the major endoplasmic reticulum transmembrane proteins with regulation on the signaling pathways of ERS. In addition, treat-

ment with delanzomib also led to the increased expression of ERS-associated proteins in HCC cells, including p-eIF2α, ATF4 and CHOP. In theory, PERK could phosphorylate eIF2α, leading to the selective translation of ATF4. Moreover, under the condition of prolonged ERS, ATF4-CHOP-mediated induction of several pro-apoptotic genes will further result the cell apoptosis [31]. CHOP is the most characteristic regulator in the transition from ERS to apoptosis and plays a key role in the ERS response as a pro-apoptotic transcriptional factor [32]. Therefore, based on our results, we speculated that during ERS induced by delanzomib in HCC cells, the ERS kinase PERK was activated, transducing the ERS signal through phosphorylation of its downstream effectors eIF2α, and increasing the expression of ATF4 and CHOP. ERS could trigger the delanzomib-induced apoptosis through the PERK/eIF2α/ATF4/CHOP pathway in both sorafenib sensitive and resistant HCC cells.

Although our present study demonstrated good pre-clinical efficacy of delanzomib on HCC, two important issues need to be noted and further studies are required. The first issue is the acquired resistance for proteasome inhibitors. Like bortezomib, acquired drug resistance is often mentioned both in pre-clinical and clinical studies [33]. The identified resistance mechanisms includes the over-expression of CIP2A/AKT pathway and proteasome subunits in HCC [22, 34]. In addition, autophagy is thought to be another cellular process associated with acquired drug resistance of proteasome inhibi-

tors [35, 36]. As we known, besides proteasome, autophagy might also contribute to degrade the unfolded proteins and engulf overloaded parts of the endoplasmic reticulum. Therefore, HCC cells might be adapted to gain advantages through the ERS-induced autophagy by keeping the cells away from apoptosis and promoting survival [27]. However, it is unclear whether the acquired resistance to delanzomib will occur in HCC and further studies are needed. Another issue needed to be noted is the tumor heterogeneity of HCC, which attributed to the different characteristics of differentiation, genetic defects, different ethnic origins and the biological behavior of HCC cell lines [37]. For example, lacking functional p53 may lead to the transient resistance and the delayed pro-apoptotic effects of proteasome inhibitors in HCC cells [38]. Therefore, the assortment of underlying pathologies combined with the inherent heterogeneity of HCC might be related to the efficacy of delanzomib in HCC clinical trials. This is also interesting worthy for indepth research.

Our study has three important implications (**Figure 7**). First, delanzomib exhibited excellent antitumor effect against HCC cell lines by inducing G2/M cell cycle arrest and cell apoptosis in vitro, and significantly suppresses HCC tumor growth in vivo with relative low systematic cytotoxicity. Second, ERS triggered delanzomib-induced apoptosis in HCC cells through the PERK/eIF2α/ATF4/CHOP pathway. Third, delanzomib remained active in sorafenib-resistant HCC cells.

In summary, to the extent of our knowledge, this is the first study to evaluate the antitumor effects of delanzomib in HCC. The results together with its known low toxicity make it possible that delanzomib might be a potential drug candidate for the patients with advanced HCC, as well as those relapsed HCC with resistence on sorafenib therapy in clinics, and worthy for further study.

Acknowledgements

Disclosure of conflict of interest

None.

Address correspondence to: Dong-Hai Jiang and Shu-Sen Zheng, Department of Surgery, Division of Hepatobiliary and Pancreatic Surgery, First Affiliated Hospital, School of Medicine, Zhejiang University, Hangzhou 310000, Zhejiang Province, China. Tel: +86-571-87236567; Fax: +86-571-87236567; E-mail: jdh8499@zju.edu.cn (DHJ); shusenzheng@zju.edu.cn (SSZ)

References

[1] Bray F, Ferlay J, Soerjomataram I, Siegel RL, Torre LA and Jemal A. Global cancer statistics 2018: GLOBOCAN estimates of incidence and mortality worldwide for 36 cancers in 185 countries. CA Cancer J Clin 2018; 68: 394-424.

[2] Chen W, Zheng R, Baade PD, Zhang S, Zeng H, Bray F, Jemal A, Yu XQ and He J. Cancer statistics in China, 2015. CA Cancer J Clin 2016; 66: 115-132.

[3] El-Serag HB. Hepatocellular carcinoma. N Engl J Med 2011; 365: 1118-1127.

[4] Chen KW, Ou TM, Hsu CW, Horng CT, Lee CC, Tsai YY, Tsai CC, Liou YS, Yang CC, Hsueh CW and Kuo WH. Current systemic treatment of hepatocellular carcinoma: a review of the literature. World J Hepatol 2015; 7: 1412-1420.

[5] Cheng AL, Kang YK, Chen Z, Tsao CJ, Qin S, Kim JS, Luo R, Feng J, Ye S, Yang TS, Xu J, Sun Y, Liang H, Liu J, Wang J, Tak WY, Pan H, Burock K, Zou J, Voliotis D and Guan Z. Efficacy and safety of sorafenib in patients in the Asia-Pacific region with advanced hepatocellular carcinoma: a phase III randomised, double-blind, placebo-controlled trial. Lancet Oncol 2009; 10: 25-34.

[6] Lencioni R, Llovet JM, Han G, Tak WY, Yang J, Guglielmi A, Paik SW, Reig M, Kim DY, Chau GY, Luca A, Del Arbol LR, Leberre MA, Niu W, Nicholson K, Meinhardt G and Bruix J. Sorafenib or placebo plus TACE with doxorubicin-eluting beads for intermediate stage HCC: the SPACE trial. J Hepatol 2016; 64: 1090-1098.

[7] Guerrero-Garcia TA, Gandolfi S, Laubach JP, Hideshima T, Chauhan D, Mitsiades C, Anderson KC and Richardson PG. The power of proteasome inhibition in multiple myeloma. Expert Rev Proteomics 2018; 15: 1033-1052.

[8] Huang IT, Dhungel B, Shrestha R, Bridle KR, Crawford DHG, Jayachandran A and Steel JC. Spotlight on Bortezomib: potential in the treatment of hepatocellular carcinoma. Expert Opin Investig Drugs 2019; 28: 7-18.

[9] Richardson PG, Mitsiades C, Hideshima T and Anderson KC. Bortezomib: proteasome inhibition as an effective anticancer therapy. Annu Rev Med 2006; 57: 33-47.

[10] Kane RC, Bross PF, Farrell AT and Pazdur R. Velcade: U.S. FDA approval for the treatment of multiple myeloma progressing on prior therapy. Oncologist 2003; 8: 508-513.

[11] Kim GP, Mahoney MR, Szydlo D, Mok TS, Marshke R, Holen K, Picus J, Boyer M, Pitot HC, Rubin J, Philip PA, Nowak A, Wright JJ and Erlichman C. An international, multicenter phase II trial of bortezomib in patients with hepatocellular carcinoma. Invest New Drugs 2012; 30: 387-394.

[12] Piva R, Ruggeri B, Williams M, Costa G, Tamagno I, Ferrero D, Giai V, Coscia M, Peola S, Massaia M, Pezzoni G, Allievi C, Pescalli N, Cassin M, di Giovine S, Nicoli P, de Feudis P, Strepponi I, Roato I, Ferracini R, Bussolati B, Camussi G, Jones-Bolin S, Hunter K, Zhao H, Neri A, Palumbo A, Berkers C, Ovaa H, Bernareggi A and Inghirami G. CEP-18770: a novel, orally active proteasome inhibitor with a tumor-selective pharmacologic profile competitive with bortezomib. Blood 2008; 111: 2765-2775.

[13] Dorsey BD, Iqbal M, Chatterjee S, Menta E, Bernardini R, Bernareggi A, Cassara PG, D'Arasmo G, Ferretti E, De Munari S, Oliva A, Pezzoni G, Allievi C, Strepponi I, Ruggeri B, Ator MA, Williams M and Mallamo JP. Discovery of a potent, selective, and orally active proteasome inhibitor for the treatment of cancer. J Med Chem 2008; 51: 1068-1072.

[14] Berkers CR, Leestemaker Y, Schuurman KG, Ruggeri B, Jones-Bolin S, Williams M and Ovaa H. Probing the specificity and activity profiles of the proteasome inhibitors bortezomib and delanzomib. Mol Pharm 2012; 9: 1126-1135.

[15] Sanchez E, Li M, Steinberg JA, Wang C, Shen J, Bonavida B, Li ZW, Chen H and Berenson JR. The proteasome inhibitor CEP-18770 enhances the anti-myeloma activity of bortezomib and melphalan. Br J Haematol 2010; 148: 569-581.

[16] Chen R, Cheng Q, Owusu-Ansah KG, Chen J, Song G, Xie H, Zhou L, Xu X, Jiang D and Zheng S. Cabazitaxel, a novel chemotherapeutic alternative for drug-resistant hepatocellular carcinoma. Am J Cancer Res 2018; 8: 1297-1306.

[17] Jiang Y, Sun A, Zhao Y, Ying W, Sun H, Yang X, Xing B, Sun W, Ren L, Hu B, Li C, Zhang L, Qin G, Zhang M, Chen N, Huang Y, Zhou J, Liu M, Zhu X, Qiu Y, Sun Y, Huang C, Yan M, Wang M, Liu W, Tian F, Xu H, Wu Z, Shi T, Zhu W, Qin J, Xie L, Fan J, Qian X and He F. Proteomics identifies new therapeutic targets of early-stage hepatocellular carcinoma. Nature 2019; 567: 257-261.

[18] Wang B, Zhou TY, Nie CH, Wan DL and Zheng SS. Bigelovin, a sesquiterpene lactone, suppresses tumor growth through inducing apoptosis and autophagy via the inhibition of mTOR pathway regulated by ROS generation in liver cancer. Biochem Biophys Res Commun 2018; 499: 156-163.

[19] Kim I, Xu W and Reed JC. Cell death and endoplasmic reticulum stress: disease relevance and therapeutic opportunities. Nat Rev Drug Discov 2008; 7: 1013-1030.

[20] Isono M, Sato A, Asano T and Okubo K. Delanzomib interacts with ritonavir synergistically to cause endoplasmic reticulum stress in renal cancer cells. Anticancer Res 2018; 38: 3493-3500.

[21] Clarke HJ, Chambers JE, Liniker E and Marciniak SJ. Endoplasmic reticulum stress in malignancy. Cancer Cell 2014; 25: 563-573.

[22] Wu YX, Yang JH and Saitsu H. Bortezomib-resistance is associated with increased levels of proteasome subunits and apoptosis-avoidance. Oncotarget 2016; 7: 77622-77634.

[23] Hou J, Cui A, Song P, Hua H, Luo T and Jiang Y. Reactive oxygen species-mediated activation of the Src-epidermal growth factor receptor-Akt signaling cascade prevents bortezomib-induced apoptosis in hepatocellular carcinoma cells. Mol Med Rep 2015; 11: 712-718.

[24] Farra R, Dapas B, Baiz D, Tonon F, Chiaretti S, Del Sal G, Rustighi A, Elvassore N, Pozzato G, Grassi M and Grassi G. Impairment of the Pin1/E2F1 axis in the anti-proliferative effect of bortezomib in hepatocellular carcinoma cells. Biochimie 2015; 112: 85-95.

[25] Niewerth D, Jansen G, Assaraf YG, Zweegman S, Kaspers GJ and Cloos J. Molecular basis of resistance to proteasome inhibitors in hematological malignancies. Drug Resist Updat 2015; 18: 18-35.

[26] Walter P and Ron D. The unfolded protein response: from stress pathway to homeostatic regulation. Science 2011; 334: 1081-1086.

[27] Riha R, Gupta-Saraf P, Bhanja P, Badkul S and Saha S. Stressed out - therapeutic implications of er stress related cancer research. Oncomedicine 2017; 2: 156-167.

[28] Boyce M and Yuan J. Cellular response to endoplasmic reticulum stress: a matter of life or death. Cell Death Differ 2006; 13: 363-373.

[29] Xu C, Bailly-Maitre B and Reed JC. Endoplasmic reticulum stress: cell life and death decisions. J Clin Invest 2005; 115: 2656-2664.

[30] Dikic I. Proteasomal and autophagic degradation systems. Annu Rev Biochem 2017; 86: 193-224.

[31] Rozpedek W, Pytel D, Mucha B, Leszczynska H, Diehl JA and Majsterek I. The role of the PERK/eIF2alpha/ATF4/CHOP signaling pathway in tumor progression during endoplasmic reticulum stress. Curr Mol Med 2016; 16: 533-544.

[32] Liu Y, Gong W, Yang ZY, Zhou XS, Gong C, Zhang TR, Wei X, Ma D, Ye F and Gao QL. Quercetin induces protective autophagy and apoptosis through ER stress via the p-STAT3/Bcl-2 axis in ovarian cancer. Apoptosis 2017; 22: 544-557.

[33] McConkey DJ and Zhu K. Mechanisms of proteasome inhibitor action and resistance in cancer. Drug Resist Updat 2008; 11: 164-179.

[34] Chen KF, Yeh PY, Hsu C, Hsu CH, Lu YS, Hsieh HP, Chen PJ and Cheng AL. Bortezomib overcomes tumor necrosis factor-related apoptosis-inducing ligand resistance in hepatocellular carcinoma cells in part through the inhibition of the phosphatidylinositol 3-kinase/Akt pathway. J Biol Chem 2009; 284: 11121-11133.

[35] Yorimitsu T, Nair U, Yang Z and Klionsky DJ. Endoplasmic reticulum stress triggers autophagy. J Biol Chem 2006; 281: 30299-30304.

[36] Wang Z, Zhu S, Zhang G and Liu S. Inhibition of autophagy enhances the anticancer activity of bortezomib in B-cell acute lymphoblastic leukemia cells. Am J Cancer Res 2015; 5: 639-650.

[37] Qiu GH, Xie X, Xu F, Shi X, Wang Y and Deng L. Distinctive pharmacological differences between liver cancer cell lines HepG2 and Hep3B. Cytotechnology 2015; 67: 1-12.

[38] Dabiri Y, Kalman S, Gurth CM, Kim JY, Mayer V and Cheng X. The essential role of TAp73 in bortezomib-induced apoptosis in p53-deficient colorectal cancer cells. Sci Rep 2017; 7: 5423.
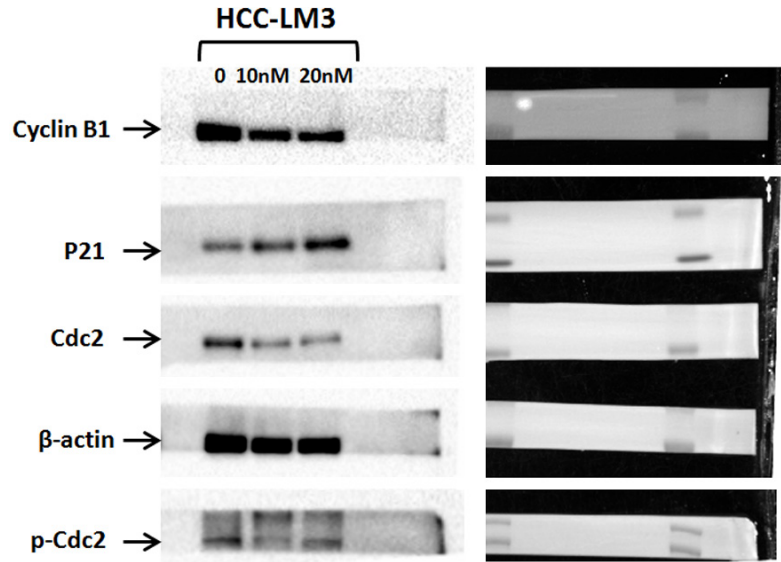
Supplementary Figure 1. The original western images for all relevant western blots including the whole membranes in **Figure 2C**.
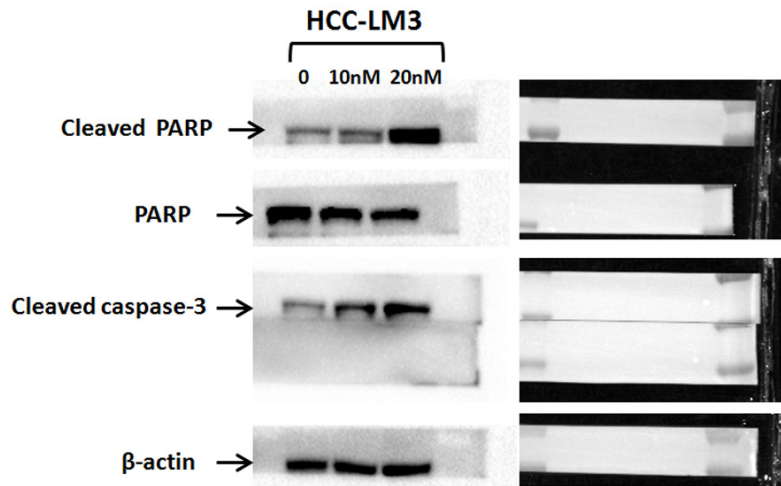
Supplementary Figure 2. The original western images for all relevant western blots including the whole membranes in **Figure 2D**.
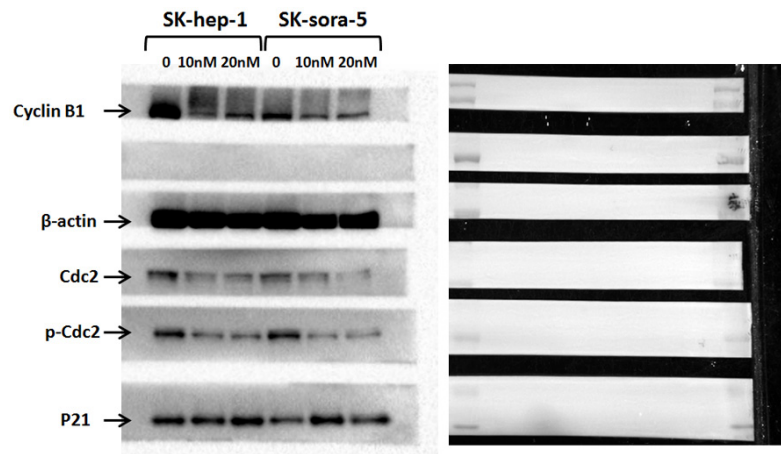
Supplementary Figure 3. The original western images for all relevant western blots including the whole membranes in **Figure 3I**.
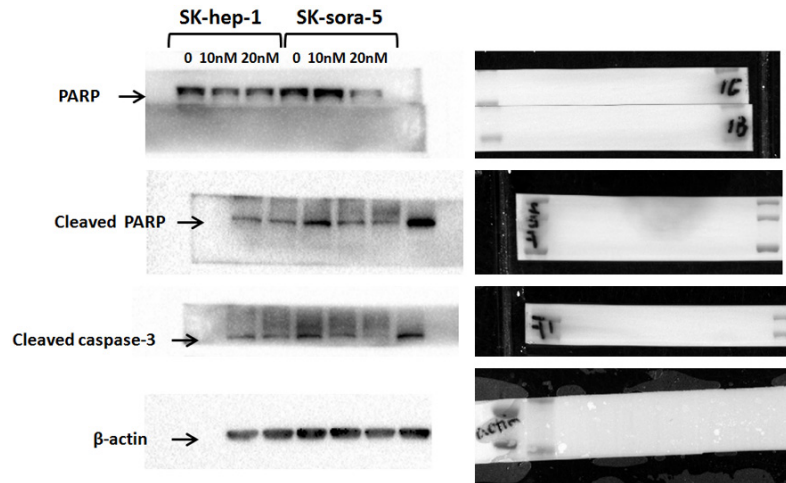
Supplementary Figure 4. The original western images for all relevant western blots including the whole membranes in **Figure 4B**.
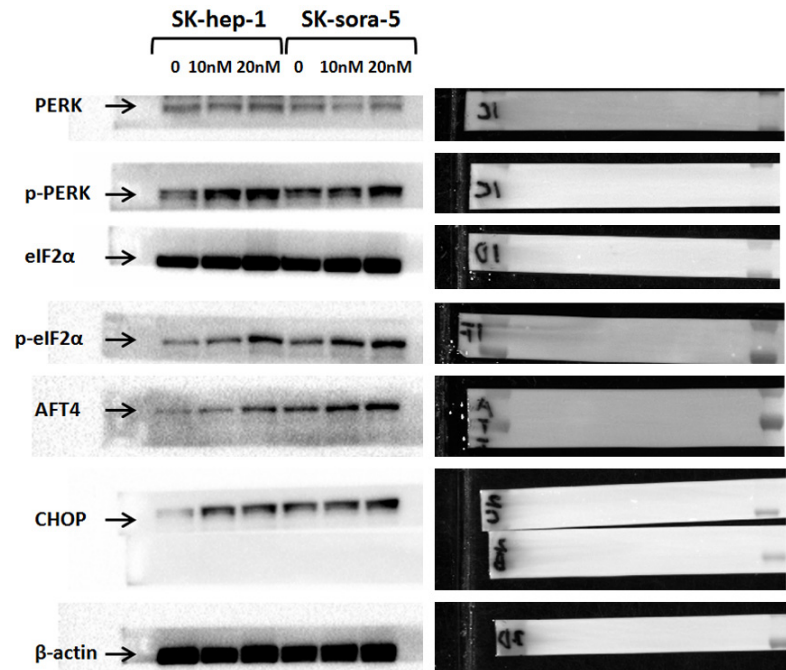
Supplementary Figure 5. The original western images for all relevant western blots including the whole membranes in **Figure 4C**.